

Study of Silane Treatment on Poly-lactic Acid(PLA)/Sepiolite Nanocomposite Thin Films

Nima Moazeni,¹ Zurina Mohamad,¹ Nazila Dehbari²

¹Department of Polymer Engineering, Faculty of Chemical Engineering, Universiti Teknologi Malaysia (UTM), Skudai, Johor, Malaysia

²Centre for NanoScale Science and Technology, School of Computer Science, Engineering and Mathematics, Flinders University, South Australia 5043, Australia

Correspondence to: N. Moazeni (E-mail: mnima2@live.utm.my or nima.moazeni@gmail.com)

ABSTRACT: Poly-lactic acid (PLA) nanocomposite film was prepared with untreated and silane treated sepiolite through solution casting method. Sepiolite is found to be promising nano inorganic filler used to prepare biodegradable PLA nanocomposite films. The effect of sepiolite loading on the thermal, mechanical, gas permeability, and water vapor permeability (WVP) properties of the films was investigated. X-ray diffraction analysis revealed the crystallinity index and well dispersed sepiolite in PLA/sepiolite thin films. By modifying sepiolite, depending on the nanoclay content, the mechanical properties of films were enhanced. PLA/sepiolite films exhibited improved gas barrier and WVP properties compared to neat PLA. The scanning electron microscope results demonstrated that there is a good interface interaction between sepiolite and PLA. The surface treatment of sepiolite increased the adhesion of the PLA matrix to the sepiolite nanoclay which yielded better mechanical properties of the films as compared to pure PLA. It was observed after 1.5% wt sepiolite, nano-filler tended to agglomerate, therefore mechanical and barrier properties of films decreased. © 2014 Wiley Periodicals, Inc. *J. Appl. Polym. Sci.* **2015**, *132*, 41428.

KEYWORDS: biodegradable; clay; composites; films

Received 23 June 2014; accepted 17 August 2014

DOI: 10.1002/app.41428

INTRODUCTION

Biodegradable polymers (films) have attracted a great deal of interest from researchers in recent years due to rising environmental concerns and strict rules of using eco-friendly materials.^{1,2} In order to reduce waste disposal problems, biodegradable material was developed using renewable resources.³ Biodegradable polymers can be made comparable to conventional polymers with some chemical modification to enhance mechanical, thermal, and barrier properties which are related to a polymer's solubility, diffusivity and permeability. A variety of biopolymers have been investigated for the development of biodegradable materials from renewable resources to substitute or complement their non-biodegradable petrochemical-based counterparts. During the past two decades the aliphatic polyesters and their copolymers with desirable properties have been widely used and among the numerous polyesters studies so far, poly-lactic acid (PLA) has proven to be the most attractive polyester as it is completely biodegradable. The lactic acid process can be obtained from inexpensive raw materials such as corn, sugar beet, sugar cane, potatoes, and other biomasses. The mechanical properties of PLA can vary considerably, ranging from soft

elastic materials to stiff high strength materials, according to various parameters such as crystallinity, polymer structure, molecular weight, material formulation (plasticizers, blend, composites, etc.), and processing.⁴ However, PLA has a very low tensile ductility and poor barrier properties to water, O₂ and CO₂, and concerning its use in packaging applications, it needs to be modified by the incorporation of fillers^{5,6} and commercial polymers such as polyethylene (PE) and polypropylene (PP), and it should be flexible and strong enough for end use applications.⁷ As a result, the mechanical and thermal properties including gas permeability (GP) and water vapor permeability (WVP) must be improved. An interesting material which has been used in recent years to enhance the properties of biodegradable polymers in terms of mechanical and thermal properties is sepiolite,⁸ which disperses easily into the polymer matrix. Sepiolite is a hydrated magnesium silicate with a high specific surface area (200–300 m²/g) and porous volume (0.4 cm³/g).^{9,10} Its structure is similar to layered clay minerals (i.e., montmorillonite), and is composed of two tetrahedral silica sheets sandwiching a central octahedral sheet containing Mg, continuing in only one direction.¹¹ The structure and morphology of fibrous

Table I. Detailed Formulations of PLA/Sepiolite Nanocomposite Films

| Formulation name | Formulation content |
|------------------|--|
| PLA | Plain PLA (control formulation) |
| 0.5% U | 0.5 wt % untreated sepiolite incorporation |
| 1.0% U | 1.0 wt % untreated sepiolite incorporation |
| 1.5% U | 1.5 wt % untreated sepiolite incorporation |
| 3.0% U | 3.0 wt % untreated sepiolite incorporation |
| 0.5% T | 0.5 wt % treated sepiolite incorporation |
| 1.0% T | 1.0 wt % treated sepiolite incorporation |
| 1.5% T | 1.5 wt % treated sepiolite incorporation |
| 3.0% T | 3.0 wt % treated sepiolite incorporation |

sepiolite based nanocomposites seem easier to control than those layered silicate nanocomposites which are the result of relatively weak interaction and small contact surface between the nano-rods.¹² Consequently, this fibrous silicate can be dispersed into the polymer matrix more uniformly than the plate-like clays.¹³

Although some studies^{4-7,13} have been conducted with a focus on the mechanical, thermal, gas transport properties of oxygen, nitrogen, and carbon dioxide in PLA homopolymer materials and other properties, at present, and to the best of our knowledge, no study has reported on modified sepiolite with PLA for the development of PLA/sepiolite nanocomposite films. This novel work presents a facile approach to environmentally friendly preparation of nanocomposite film based on PLA and modified and unmodified sepiolite which can be used potentially as food packaging films as a final application. The morphology, thermal stability, GP, water absorption, and mechanical properties of the films were also studied.

EXPERIMENTAL

Materials

PLA was supplied by Nature Works LLC in the form of granules with a density of 1.31 g/cm³. Sepiolite (with average original diameter size of 100 nm) was supplied by Shijiazhuang Kedahua Imp & Exp. Trade Co. (Hebei, China) in powder form with no chemical treatment prior to processing. The silane was used as the filler surface modifying coupling agent and was purchased from Gelest Inc. Morrisville, PA.

Silane Treatment

For the surface-treatment of the sepiolite, 5 wt % (3-Amino-propyl) trimethoxysilane was dissolved in a mixture of ethanol-water (60 : 40 w/w). The solution was stirred continuously for 1 h and its pH was adjusted to 4 with acetic acid. Next, sepiolite was soaked in the solution for 3 h. It was then washed with distilled water and kept in air for 3 days prior to oven drying at 80°C for 12 h.¹⁴

Preparation of Poly-Lactic Acid (PLA)/Sepiolite Film

PLA/sepiolite films were obtained by the solution casting method. First, 5 g of PLA (MW: 100,000, Polyscience Inc, PA, 18976) was dissolved in 100 mL of chloroform (Sigma C-5312;

St. Louis). Normal and modified sepiolite in different amounts (0.5, 1, 1.5, and 3 wt %) were dispersed in chloroform for 30 min using a sonicator (Model FB15053; Fisher Scientific Co., Germany). The solution was then mixed for 24 h at 85°C before de-bubbling using a sonicator for 10 min in ambient temperature. The solution was then placed in glass plates, and with the use of a Gardner casting blade, PLA film was made. After solvent evaporation, the films were dried at 25°C and were kept in a desiccator. The mean thickness was 40 μm. Table I shows the primer formulation of the PLA/sepiolite nanocomposite film recipes that were used in this study.

Characterization

To evaluate the interaction between sepiolite and PLA matrix and also to investigate the effect of sepiolite content on the crystallinity of polymer membranes, an X-ray diffractometer (SIEMEN D500, Germany) was employed. The test was conducted at room temperature. The scattering angles were measured within the range of 10° to 50° (2θ) (step size = 0.02°, scanning rate = 2 s/step) with 40 kV power using filtered Cu Kα radiation (λ = 1.5406Å). The crystallinity index, *I_c* is determined by this formula:¹⁵

$$I_c = \left[1 - \left(\frac{I_{min}}{I_{max}} \right) \right] \times 100\%$$

where *I_{min}* and *I_{max}* are the intensity value at lower and higher peaks, respectively.

The melting point (*T_m*), heat of fusion, Δ*H*, and the crystallinity of the PLA/sepiolite films were measured on a Perkin-Elmer DSC 7 differential scanning calorimeter. The samples weighed 7 mg and the heating rate was set at 10°C/min (under nitrogen flow). *T_m* and Δ*H* were calibrated with indium. The samples were first scanned from 30 to 250°C and then held at this temperature for 5 minutes before cooling to 30°C.

The degree of crystallinity (*X_c*) of the PLA/sepiolite nanocomposite film was estimated by

$$X_c = \frac{\Delta H_f 100}{\Delta H_f^0 (1 - \emptyset)}$$

where Δ*H_f* is the heat of fusion of the PLA and composites, Δ*H_f*⁰ is the heat of fusion for 100% crystalline PLA (Δ*H*100 = 93.7 J/g), and ∅ is the filler fraction.¹⁶

The tensile properties of PLA/sepiolite film were measured using Universal Testing Machine (UTM; Lloyd Instruments, Press Motor Hydraulic Lab Press Gutrie M' SIA) at 10 mm/min cross head speed according to ASTM D882-10 at 25°C. Elongation-at-break was also calculated as the ratio of the final length at the point of sample rupture to the initial length of a specimen, which was repeated on at least five samples of each membrane. Average values were then reported. All measurements were performed at 25°C with a relative humidity of 60%.

The permeability coefficient (*P*) of pure gases [oxygen (O₂) and carbon dioxide (CO₂)] in the PLA/sepiolite nanocomposite films was determined using a constant pressure method and soap bubble flow meter. The feed pressure was 5 bar and the permeate side was maintained under vacuum at 25°C. All

results were determined for three samples. The pure GP was calculated by using the equation below:

$$P = \frac{l}{A\Delta p} \frac{dV}{dt}$$

where P is the permeability, l is the film thickness (m), Δp is the pressure difference across films (Pa), A is the effective surface area ($12.5 \times 10^{-4} \text{ m}^2$), V is the volume of the gas permeated through the membrane [$\text{m}^3(\text{STP})$] and t is the permeation time (s).¹⁷

Using WVP measurements, the mass fabric transfer was measured following the guidelines of ASTM E 96-80B. Round mouth conical plastic cups with diameter of 25 mm and a height of 90 mm were filled with distilled water. The membrane samples were placed over the top of the cups and completely sealed. The gap between the fabric and water surface was about 4 mm. Cups were placed in a constant temperature chamber. During all WVP measurements, air surrounding the fabric had a constant temperature and a relative humidity of 70%. For each WVP measurement, three different samples were used, which are calculated by using the following formula:

$$WVP = \frac{(WVTR \times L)}{\Delta p}$$

where WVTR is the water vapor transmission rate ($\text{g}/\text{m}^2 \cdot \text{s}$) measured through a film, Δp is the partial water vapor pressure difference (Pa) across the two sides of the film, and L is the mean film thickness (m).

The surface and cross sectional structures (cryogenically fractured surface) of the PLA/sepiolite films were observed and dispersion and distribution of nano-fillers in PLA matrix in films were investigated by using scanning electron microscope (SEM) (JEOL JSM-6380LA). All samples were coated with a thin layer of gold for 1 min at 1.4 V to avoid electrostatic discharge during the examination. The tested samples were prepared by cutting prepared film into 2×2 cm pieces. Prior to observation, samples were placed into liquid nitrogen and broken.

RESULTS AND DISCUSSION

X-ray Diffraction Analysis

Figure 1(A) shows the pure sepiolite, Figure 1(B,C) show the XRD pattern on PLA/sepiolite nanocomposite film with and without treatment, respectively. XRD data is used to investigate the interaction between sepiolite filler and PLA matrix and also to assess the effect of sepiolite content on the crystallinity of the polymer matrix. As seen in Figure 1(A), pure sepiolite is characterized by peaks (154) (38) (82) (180) (261), and (75) planes corresponding to the $2\Theta = 10.55^\circ$, 19.70° , 27.25° , 28.60° , 29.45° , and 33.15° . The sepiolite characteristic peak in PLA/sepiolite films disappeared [Figure 1(B,C)] except for (154) (261), and (75) planes corresponding to $2\Theta = 10.55^\circ$, 29.45° , and 33.15° which indicates that the sepiolite bundles are generally delaminated to stick to filler and are dispersed homogeneously into the PLA matrix which suggests that parallel form of sepiolite stacking was totally disrupted which gives an indication of sepiolite exfoliation into PLA matrix.¹⁸ This result may be due to the interaction between silanol groups (Si—OH) on

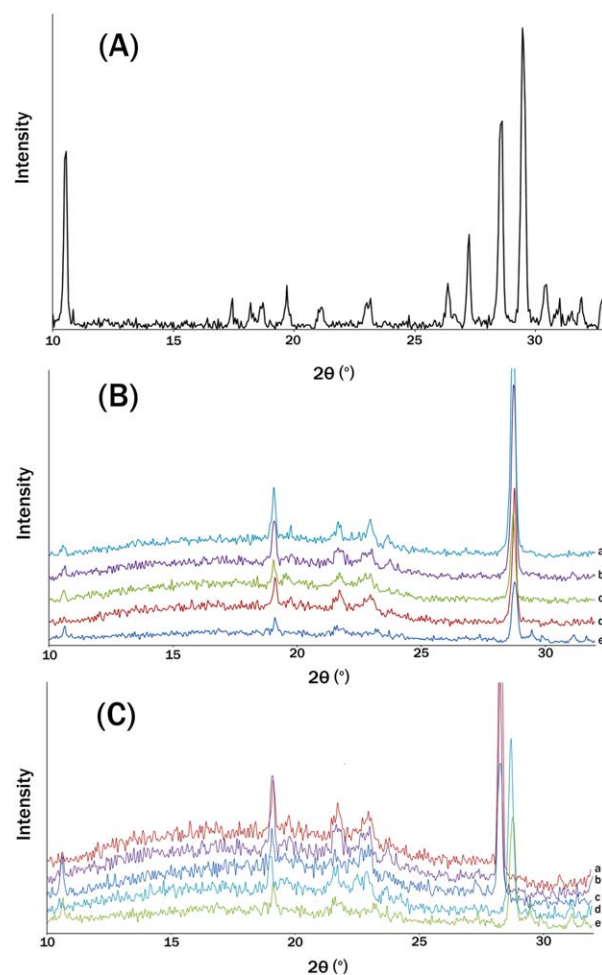


Figure 1. XRD data. (A) XRD pattern of Sepiolite powder. (B) Comparison of Untreated Sepiolite/PLA. [Color figure can be viewed in the online issue, which is available at wileyonlinelibrary.com.]

sepiolite and the ester groups of PLA.¹⁹ The crystallinity index for PLA/sepiolite nanocomposite films at different sepiolite content with and without treatment was gathered in Table II.

From Table II, the highest crystallinity index is for 1.5 wt % sepiolite loading. A possible reason is that the sepiolite acts as the nucleating agent to promote polymer crystallite growth if they were initiated on the sepiolite surface or between the sepiolite fillers. The same trend was obvious for silane treated nanocomposites; however it can be implied from Table II that the modified sepiolite imparts better properties regarding higher induced crystallinity. Highest crystallinity was achieved with 1.5 wt % treated sepiolite (50.87%) which is 9% higher compared to untreated sepiolite. This can be attributed to the improvement in interaction between sepiolite and PLA by applying treatment.

It is obvious in Table II that imparting sepiolite in PLA matrix increases crystallinity up to 1.5 wt % sepiolite incorporation which is also supported by DSC data Table III and may be due to the fact that sepiolite content can act as a nucleating agent in the matrix. So here, the surface roughness of sepiolite is expected to initiate the growth of crystals on PLA/sepiolite

Table II. Crystallinity Index of Treated and Untreated Sepiolite/PLA Nanocomposite Films

| Formulation | Crystallinity index (%) |
|-------------|-------------------------|
| PLA | 31.12 |
| 0.5% U | 33.20 |
| 1.0% U | 40.71 |
| 1.5% U | 41.43 |
| 3.0% U | 39.21 |
| PLA | 31.12 |
| 0.5% T | 34.93 |
| 1.0% T | 42.19 |
| 1.5% T | 50.87 |
| 3.0% T | 39.88 |

inter-phase. At higher sepiolite loading (3 wt %), filler–filler interaction becomes more pronounced than filler–matrix interaction and filler particles tend to agglomerate, so as a result, the degree of crystallinity decreases due to the reduced effectiveness of the cross sectional area of the nanocomposite film caused by sepiolite particles.

Differential Scanning Calorimeter (DSC)

The thermal transition properties of the PLA with treated and untreated sepiolite films were investigated with differential scanning calorimetry (DSC) and are shown in Figure 2 and Table III. It can be seen that by incorporation of sepiolite into the PLA matrix T_g increases linearly from 52.39°C for pure PLA to 62.54°C for 3 wt % sepiolite. T_g is related to the relative density of the amorphous and crystalline states. Most often the more orderly crystalline state has the higher density at T_g and the non-crystalline molecular chains are constrained as they are anchored to the immobile crystallites, increasing T_g .²⁰ The same trend was observed for T_m .

From differential scanning calorimetry (DSC) measurements, a slight change in crystallinity was measured owing to the nucleating effect induced by the sepiolite. The sepiolite fillers act as

Table III. DSC Comparison Data of Treated and Untreated Sepiolite/PLA Nanocomposite Films

| Formulation | T_g | T_m | ΔH_m | ΔH_c | X_c (%) |
|-------------|-------|--------|--------------|--------------|-----------|
| PLA | 52.39 | 136.17 | 13.087 | 11.134 | 25.85 |
| 0.5% U | 52.88 | 136.61 | 13.421 | 11.119 | 26.19 |
| 1.0% U | 61.35 | 137.12 | 14.116 | 11.279 | 27.10 |
| 1.5% U | 61.86 | 137.48 | 14.896 | 11.405 | 28.06 |
| 3.0% U | 62.54 | 138.50 | 13.416 | 11.133 | 26.20 |
| PLA | 52.39 | 136.17 | 13.087 | 11.134 | 25.85 |
| 0.5% T | 52.80 | 136.68 | 15.141 | 11.147 | 28.05 |
| 1.0% T | 61.34 | 137.33 | 15.575 | 13.923 | 31.13 |
| 1.5% T | 61.90 | 137.67 | 17.313 | 19.351 | 39.14 |
| 3.0% T | 62.65 | 138.83 | 14.954 | 11.435 | 28.16 |

hetero-phase nucleating agents.²¹ In fact, the incorporation of nano-fillers in a polymer matrix usually causes an increase in the glass transition temperature which is explained by the confinement effect which reduces macromolecular chain mobility.²² The good interaction between PLA and sepiolite as proven by XRD data also influences chain mobility thus increasing the T_g value of nanocomposite film as sepiolite content increases.

X_c was observed to increase up to 1.5 % sepiolite (28.06%) followed by a decrease to 26.2% observed for 3% sepiolite which can be attributed to the tendency of sepiolite nanoclay to agglomerate. SEM results (Figure 5) also showed this trend and proved that agglomeration occurs after 1.5%.

Treated sepiolite shows the same trend but with a bit higher degree of crystallinity from 25.85 to 39.14% for neat PLA to 1.5% sepiolite, respectively, which can be attributed to the better interaction between matrix and filler. It shows that the addition of silane treated sepiolite influenced the thermal events and crystallinity. This increment was about 10°C in T_g , 2°C in T_m and about 14% in X_c from neat PLA to 1.5% silane treated sepiolite. However, compared with untreated sepiolite, this change was about 9°C in T_g , 1.5°C in T_m and 3% from neat

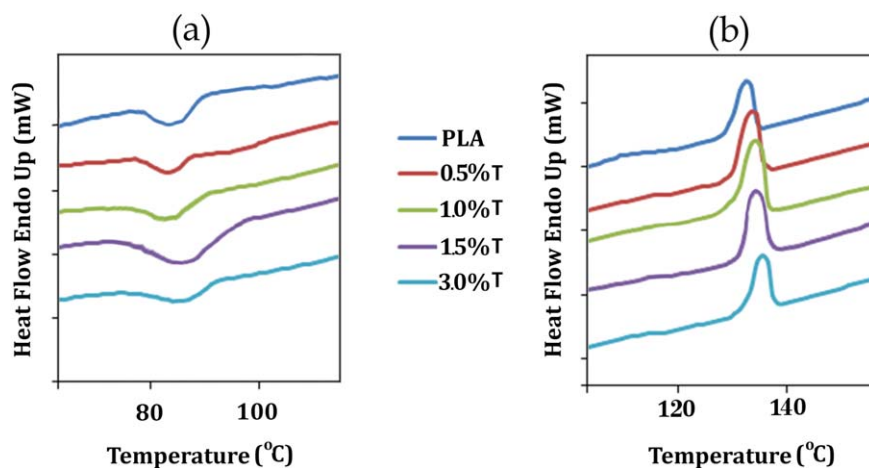


Figure 2. DCS data. (a) Comparison of crystallization peaks of DSC graph. (b) Comparison of melting point. [Color figure can be viewed in the online issue, which is available at wileyonlinelibrary.com.]

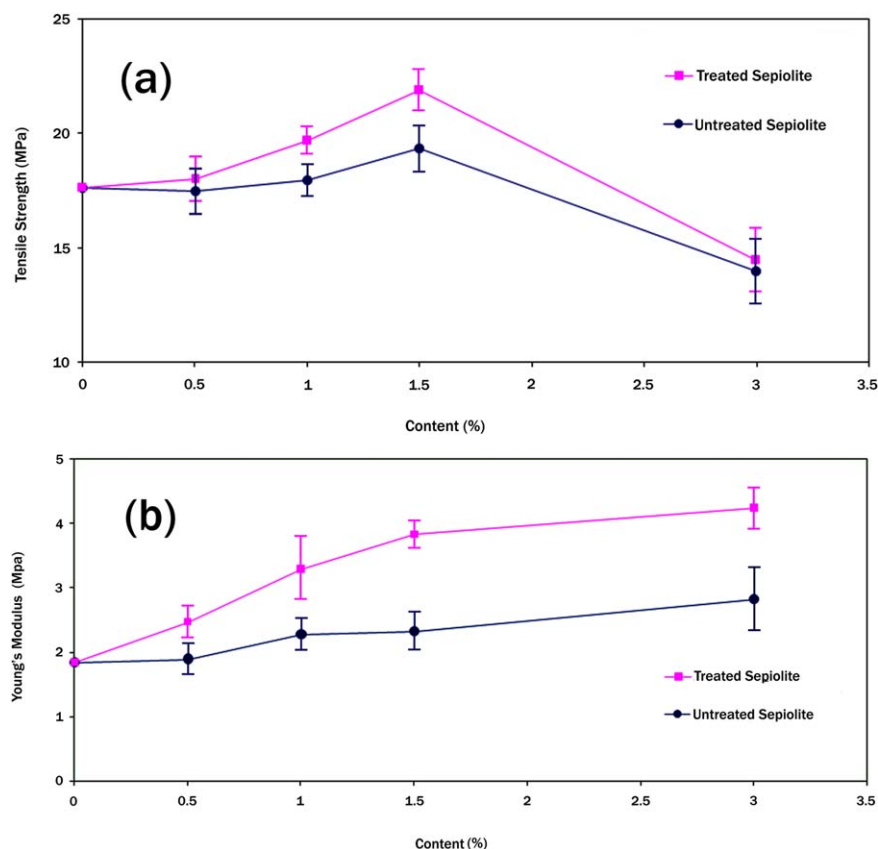


Figure 3. Mechanical properties. (a) Comparison of tensile strength of untreated and treated Sepiolite/PLA nanocomposite films. (b) Comparison of Young's Modulus of untreated and treated sepiolite/PLA nanocomposite films. [Color figure can be viewed in the online issue, which is available at wileyonlinelibrary.com.]

PLA to 1.5% sepiolite. Better interaction can cause better distribution and as sepiolite can act as a nucleating agent in matrix, it can impart more crystallinity to the composite which is about 11% higher than untreated sepiolite with 1.5 wt % incorporation. A higher crystallinity percentage led to the increment of melting temperature (T_m). On the other hand, T_g is increased which is believed to be due to the enhanced interaction between PLA and sepiolite with silane treatment.

Mechanical Properties

Figure 3(a) shows the effect of sepiolite content on tensile strength of PLA with untreated sepiolite and silane treated sepiolite nanocomposite film. It can be observed that the addition of untreated sepiolite increased the tensile strength of the PLA films from 17.63 to 19.36 Mpa for neat PLA and 1.5% sepiolite, respectively, and the treatment of sepiolite can fortify this increment up to 21.9 Mpa with 1.5% silane treated sepiolite which was much higher than that of neat PLA. Normally, the individual nature of the filler determines the tensile strength of the bio-composites.²³ In addition, the shape of sepiolite (needle like) with high aspect ratio leads to a more efficient stress transfer when a load is applied to the nanocomposites, and as a result a stronger material is formed. As sepiolite loading increased further (3 wt %), tensile strength decreased, which is attributed to the aggregation of sepiolite particles. Previous

studies also reported that high nanoclay content (e.g. MMT) (>5 wt %) in polymer can result in its agglomeration resulting in reduced mechanical performance compared to lower content.^{24,25} Moreover, high sepiolite nanoclay content can increase the brittleness of materials, making the matrix stiffer with less plastic in deformation, which are typical characteristics of hard inorganic phase. Silane treatment of sepiolite had imparted a good stress transfer from matrix to filler due to the better interaction between sepiolite and PLA which can cause further increment in tensile strength of PLA/sepiolite film.

Figure 3(b) illustrates the dependence of Young's modulus on the sepiolite content. The Young's modulus of PLA films increased linearly with increasing sepiolite loadings. All the nanocomposite films exhibited about 40% increase in modulus compare to the pure PLA films. The improvement in PLA modulus is due to the high rigidity exerted by the sepiolite as it does not deform or relax, and therefore the PLA's chain movement was suppressed by sepiolite particles. This improvement in modulus is more pronounced by silane treatment of sepiolite which may be ascribed to the better dispersion and adhesion of sepiolite particles within PLA. It can be assumed that silane treatment of sepiolite can provide a larger interfacial region with more effective stress transfer from PLA matrix to sepiolite nanoclay.

Table IV. Gas Permeability

| (A) | Oxygen permeability (10^{-17} m ³ m/m ² s Pa) | Oxygen permeability (10^{-17} m ³ m/m ² s Pa) | |
|--------|---|---|-------------|
| PLA | 0.37 ± 0.04 | PLA | 0.37 ± 0.06 |
| 0.5% U | 0.21 ± 0.10 | 0.5% T | 0.19 ± 0.04 |
| 1.0% U | 0.12 ± 0.13 | 1.0% T | 0.11 ± 0.09 |
| 1.5% U | 0.07 ± 0.11 | 1.5% T | 0.04 ± 0.13 |
| 3.0% U | 0.11 ± 0.07 | 3.0% T | 0.10 ± 0.10 |
| (B) | CO ₂ permeability (10^{-17} m ³ m/m ² s Pa) | CO ₂ permeability (10^{-17} m ³ m/m ² s Pa) | |
| PLA | 1.87 ± 0.09 | PLA | 1.87 ± 0.07 |
| 0.5% U | 1.46 ± 0.05 | 0.5% T | 1.40 ± 0.06 |
| 1.0% U | 1.34 ± 0.08 | 1.0% T | 1.29 ± 0.11 |
| 1.5% U | 1.19 ± 0.12 | 1.5% T | 1.07 ± 0.09 |
| 3.0% U | 1.32 ± 0.14 | 3.0% T | 1.30 ± 0.10 |

Gas Permeability

Carbon dioxide and oxygen permeation results for treated and untreated sepiolite and neat PLA are gathered in Table IV. A polymers GP coefficient usually follows this order: $PO_2 < PCO_2^{26}$ and $DCO_2 < DO_2$ (P = Permeability, D = Diffusion)²⁷ according to the diameter of the molecules ($dCO_2 = 0.39 \times 10^{-2}$ nm $>$ $dO_2 = 0.35 \times 10^{-2}$ nm).²⁸ Gas barrier properties are reported to be strongly dependent on shape, presence and dispersion of nanoclays as well as level of crystallinity, measurement temperature and feed gas pressure.^{28–30} By extensive dispersion of the sepiolite into PLA up to 1.5 wt % loading, the barrier properties of O_2 and CO_2 improved from 0.37×10^{17} to 0.07×10^{17} and from 1.87×10^{17} to 1.19×10^{17} , respectively. However, by increasing the amount of sepiolite into PLA the permeation of O_2 and CO_2 from the films decreased by about 0.04 (for O_2) and 0.13 (for CO_2).

The results were expected due to the formation of crystallinity in composite up to 1.5 wt % sepiolite for both treated and untreated, as well as aggregates for 3 wt % sepiolite. It is worth noting that the permeability values of O_2 and CO_2 for silane

treated sepiolite film are slightly lower than untreated sepiolite film. By increasing sepiolite content up to 1.5 wt % into PLA matrix, the GP of the films decreased by about 0.33 (O_2) and 0.8 (CO_2) as increments of effective surface area between sepiolite and PLA and as the agglomeration was forming (above 1.5 wt % sepiolite content), the free space (free volume) between filler and matrix increased and as a result O_2 and CO_2 permeability of thin film was increased by about 0.06 and 0.23 for O_2 and CO_2 , respectively. The permeability of O_2 and CO_2 of treated and untreated PLA/sepiolite films was also in agreement with the formation of crystallinity. The increment in crystallinity up to 1.5 wt % sepiolite incorporation had also reduced the O_2 and CO_2 GP, which increased afterward at 3 wt % sepiolite due to the reduction in crystallinity.

Gas permeation through a polymeric film is governed by four steps: the sorption of gas molecules on the film surface, the dissolution of the gas in the polymer, the diffusion of the gas through it and finally, desorption of the gas from the other surface of the film.³¹ Usually the amorphous polymer phase is responsible for GP through a film. Therefore for semi-crystalline polymer permeable amorphous phase dispersed in an impermeable crystalline phase. So, any increase in crystallinity leads to a decrease in GP due to a diminished contribution of the permeable amorphous phase and to an enhanced tortuosity of the diffusion path. Najafi et al. (2012)³² reported that the mechanism of gas permeation in a nanoclay reinforced polymer is similar to that in a semi-crystalline polymer.

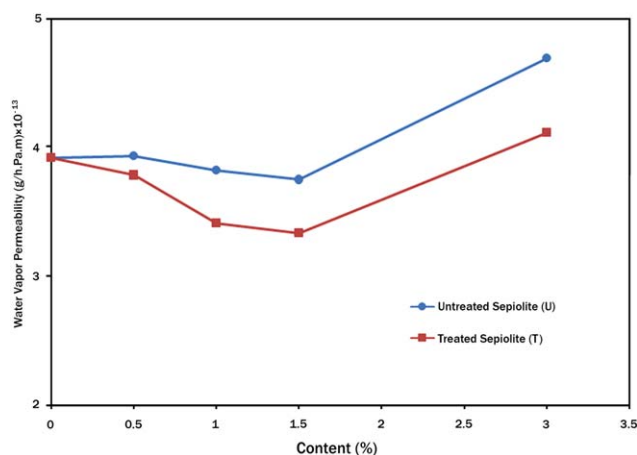


Figure 4. Comparison of water vapor permeability of untreated and treated sepiolite/PLA nanocomposite films. [Color figure can be viewed in the online issue, which is available at wileyonlinelibrary.com.]

Water Vapor Permeability

WVP test was performed on treated and untreated PLA/sepiolite films. Using the WVP equation for obtained data, the WVP curves were deduced and are shown in Figure 4. As observed in both curves, WVP of films decreased from about 4 to 3.74 (untreated sepiolite) and from about 4 to 3.33 (treated sepiolite) with increasing sepiolite content up to 1.5% which shows good interaction between matrix and filler through the crystallinity and formation of hydrogen bonding between carbonyl groups of PLA and hydroxyl groups of sepiolite.^{28,33,34} Also, at higher sepiolite loading, both silane treated and untreated

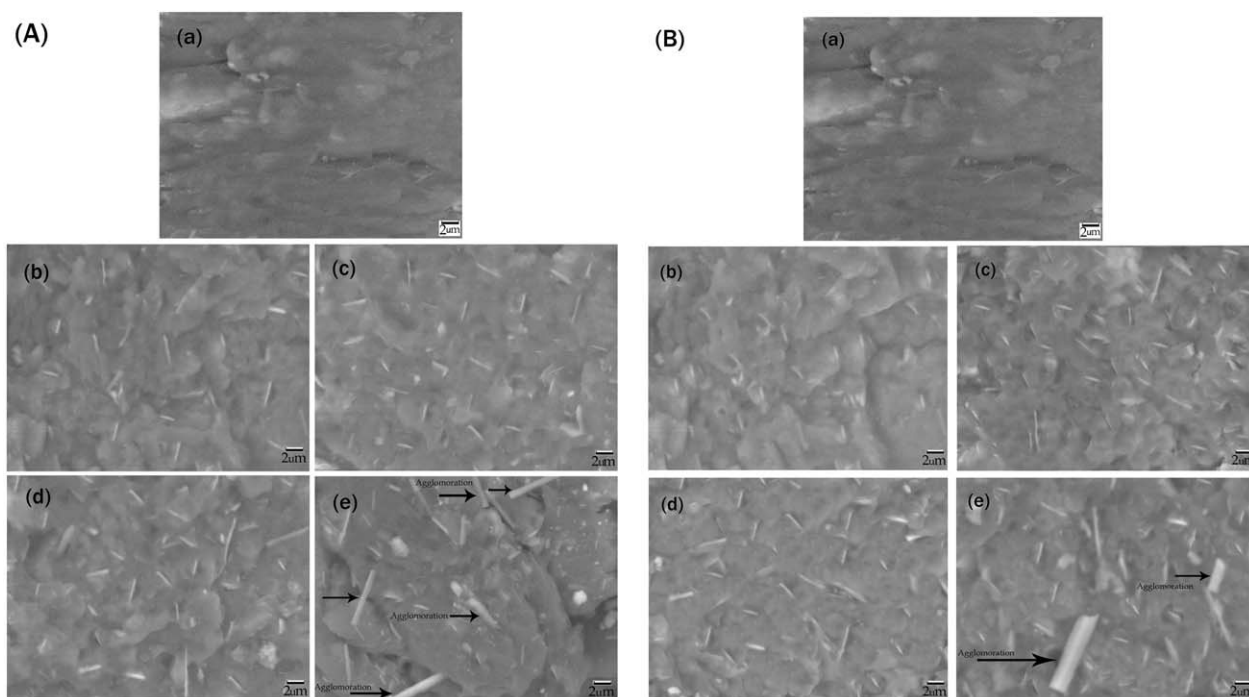


Figure 5. (A) Comparison of untreated and treated sepiolite/PLA nanocomposite films SEM: (a) PLA, (b) 0.5% U, (c) 1% U, (d) 1.5% U, (e) 3% U. (B) Comparison of untreated and treated sepiolite/PLA nanocomposite films SEM: (a) PLA, (b) 0.5% T, (c) 1% T, (d) 1.5% T, (e) 3% T.

sepiolite particles tended to aggregate, therefore WVP increased by about 23 and 25%, respectively.

Scanning Electron Microscopy (SEM)

Figure 5(A) depicts the morphology of the untreated PLA/sepiolite thin film. A good degree of sepiolite dispersion in the PLA can be observed. Sepiolite fillers are well trapped by the PLA matrix up to 1.5% loading of sepiolite content. This facilitates good adhesion between sepiolite and PLA matrix^{28,33} and is in agreement with XRD data. SEM micrographs of the silane treated films are shown in Figure 5. According to Figure 5(B) the surface of sepiolite fillers have been linking to the PLA matrix and covered with it. It was deduced that the silane causes a better wetting of the sepiolite fillers through the PLA matrix and as a result this improved adhesion leads to better stress transfer from matrix to filler and shows an increasing in tensile properties as well as improvement in GP and WVP. Both Figures shows low adherence between fillers and matrix in the case of 3 wt % sepiolite content which may due to the presence of some aggregation at the samples surface. These aggregates are distributed into the polymer matrix.

CONCLUSIONS

The T_g and T_m of PLA were slightly affected by sepiolite nanoclay. Adding sepiolite to the PLA results in PLA nucleated with a slightly higher degree of crystallinity than that of neat PLA. The maximum increase in thermal properties is registered for silane treated sepiolite film with 3 wt % sepiolite content. The incorporation of 1.5% wt silane treated sepiolite was found to be optimum as it has the highest tensile strength. The tensile modulus increased greatly according to the sepiolite content

with a reduction in the elongation at break. In terms of oxygen and carbon dioxide barrier properties, the best performance was observed for the PLA/silane treated sepiolite film with 1.5 wt % loading because of the better dispersion and interaction of the sepiolite nano-filler (nanoclay) within the PLA matrix. In case of water barrier or WVP properties, the water permeation process put forward an important barrier improvement up to 1.5 wt % increase in sepiolite (treated and untreated) content. Finally, the SEM images of the fracture surfaces obtained complied with the experimental values obtained for the samples, indicating that the incorporation of sepiolite in PLA presented good levels of dispersion. Using silane treatment of sepiolite implies that changes in surface topography affect interfacial adhesion. Above 1.5 wt % sepiolite nanoclay, some aggregates were observed on the sample fracture surface.

REFERENCES

- Han, D.; Yan, L.; Chen, W.; Li, W.; Bangal, P. R. *Carbohydr. Polym.* **2011**, *83*, 966.
- Moghaddam, M. S.; Wahit, M. U. *Int. J. Biol. Macromol.* **2013**, *58*, 133.
- Dehbari, N.; Moazeni, N.; Wan AbdulRahman, W. A. *Polym. Compos.* **2014**, *35*, 1220.
- Anne, B. *Integr. Waste Manag.* **2011**, *1*, 341.
- Gupta, A. P.; Kumar, V.; *Eur. Polym. J.* **2007**, *43*, 4053.
- Garlotta, D. *J. Polym. Environ.* **2001**, *9*, 63.
- Arvanitoyannis, I.; Nakayama, A.; Psomiadou, E.; Kawasaki, N.; Yamamoto, N. *Polymer* **1996**, *37*, 651.

8. Fukushima, K.; Tabuani, D.; Camino, G. *Mat. Sci. Eng.* **2009**, *29*, 1433.
9. Aranda, P.; Kun, R.; Martín-Luengo, M. A.; Letaïef, S.; Dékány, I.; Ruiz-Hitzky, E. *Chem. Mat.* **2008**, *20*, 84.
10. Volle, N.; Challier, L.; Burr, A.; Giulieri, F.; Pagnotta, S.; Chaze, A. M. *Comp. Sci. Tech.* **2011**, *71*, 1685.
11. Bilotti, E.; Fischer, H. R.; Peijs, T. *J. Appl. Polym. Sci.* **2008**, *107*, 1116.
12. Lu, H.; Shen, H.; Song, Z.; Shing, K. S.; Tao, W.; Nutt, S. *Macromol. Rapid. Comm.* **2005**, *26*, 1445.
13. Liu, M.; Pu, M.; Ma, H. *Comp. Sci. Tech.* **2012**, *72*, 1508.
14. Huda, M. S.; Drzal, L. T.; Mohanty, A. K.; Misra, M. *Comp. Sci. Tech.* **2008**, *68*, 424.
15. Yoon, J.; Kim, Y. *The Microbiological Society of Korea* **2005**, *43*, 487.
16. Liao, R. G.; Yang, B.; Yu, W.; Zhou, C. X. *J. Appl. Polym. Sci.* **2007**, *104*, 310.
17. Wang, L. H.; Sheng, J. *J. Macromol. Sci. Phys.* **2005**, *44*, 31.
18. Mahmoudian, S.; Wahit, M. U.; Ismail, A. F.; Yussuf, A. A. *Carbohyd. Polym.* **2012**, *88*, 1251.
19. Meitang, L.; Minfeng, P.; Hongwen, M. *Compos. Sci. Tech.* **2012**, *72*, 1508.
20. Islama, M. S.; Pickeringa, K. L.; Foremanb, N. J. *Compos. Part A: Appl. Sci. Manuf.* **2010**, *41*, 596.
21. Sanchez-Garcia, M. D.; Lopez-Rubio, A.; Lagaron, J. M. *Trends Food Sci. Technol.* **2010**, *21*, 528.
22. Tenn, N.; Follain, N.; Soulestin, J.; Crétois, R.; Bourbigot, S.; Marais, S. *J. phys. Chem. C* **2013**, *23*, 12117.
23. Kumar, R.; Yakabu, M. K.; Anandjiwala, R. D. *Compos.: Part A: Appl. Sci. Manuf.* **2010**, *11*, 1620.
24. Lee, J.; Sun, Q.; Deng, Y. *J. Biobased Mater. Bio.* **2008**, *2*, 162.
25. Wilkinson, A. N.; Man, Z.; Stanford, J. L.; Matikainen, P.; Clemens, M. L.; Lees, G. C. *Comp. Sci. Tech.* **2007**, *67*, 3360.
26. Van, K. D. W. *Properties of Polymers*, 3rd ed.; Elsevier: Amsterdam, **1997**.
27. Lebrun, L.; Bruzard, S.; Grohens, Y.; Langevin, D. *Europ. Polym. J.* **2006**, *42*, 1975.
28. Cammarano, I. S. Thesis: Study of annealing and orientation effects on physical properties of PLA based nanocomposite films. Dottotato di ricerca in ingegneria dei materiali e delle strutture XXIII ciclo, Università degli studi di Napoli Federico II. **2010**.
29. Paul, D. R.; Yampolskii, Y. P. *Polymeric Gas Separation Membranes*; CRC, Boca Raton Taylor & Francis, Technology & Engineering. **1994**.
30. Baker, R. W. *Membrane Technology and Applications*; New York: McGraw-Hill, **2000**.
31. Choudalakis, G.; Gotsis, A. D. *Europ. Polym. J.* **2010**, *45*, 967.
32. Najafi, N.; Heuzey, M. C.; Carreau, P. J. *Comp. Sci. Tech.* **2012**, *72*, 608.
33. Nunez, K.; Rosales, C.; Perera, R.; Villarreal, N.; Pastor, J. M. *Polym. Eng. Sci.* **2011**, *1*, 12.
34. Mondal, S.; Hu, J. L. *Carbohyd. Polym.* **2007**, *67*, 282.